Reconstruction of Au(111) Following the Reductive Desorption of Self-Assembled Monolayers of 2-Mercaptoethanesulfonic Acid Studied by in Situ Scanning Tunneling Microscopy

Daisuke Hobara, Masahiro Yamamoto, and Takashi Kakiuchi*
Department of Energy and Hydrocarbon Chemistry, Graduate School of Engineering, Kyoto University, Kyoto 606-8501

(Received January 11, 2001; CL-010026)

The reconstruction of Au(111) to ($\sqrt{3} \times 23$) structure after the reductive desorption of a self-assembled monolayer (SAM) composed of 2-mercaptoethanesulfonic acid (MESA) has been imaged by in situ scanning tunneling microscopy (STM) in a 0.5 mol dm^{-3} KOH aqueous solution. The STM images clearly show that after the reductive desorption of MESA the Au(111) surface reconstructs to the ($\sqrt{3} \times 23$) structure. The reconstruction starts from the edge, spreads gradually, and covers the entire terraces of Au(111) on the time scale of several minutes. Pits of the gold substrate are formed especially at the boundaries between the unreconstructed and the reconstructed areas during the spread of the reconstruction.

The reductive desorption of self-assembled monolayers (SAMs) of thiol derivatives has been utilized for the characterization and the control of the structure of thiol SAMs.[1–5] We previously showed that the morphological change of the SAM after the reductive desorption on Au(111) depends on the amphiphilic property of the desorbed thiolates.[6] Besides the morphological change of the SAMs, the structural change of the Au substrates should take place, as Au(111) is known to reconstruct into ($\sqrt{3} \times 23$) in vacuum,[7,8] in air,[9] and in solutions.[9,10] The presence of the reconstruction after the reductive desorption of SAMs is important especially to understand the re-adsorption of the desorbed thiol molecules and the adsorption of other molecules on the area where the thiol SAM was initially formed.[11,12] The elbow position of the herringbone-like ($\sqrt{3} \times 23$) reconstruction has been found to be reactive to the adsorption of various molecules.[13–15] However, no observation has been reported on the reconstruction process after the desorption. We report here the structural change of Au(111) surface accompanied by the reductive desorption of a thiol SAM. The surface structure of the SAM was studied using in situ scanning tunneling microscopy (STM)[6,16–21] in 0.5 mol dm^{-3} aqueous KOH.

2-Mercaptoethanesulfonic acid (MESA), sodium salt (Aldrich) was used without further purification. All other chemicals used were of reagent grade. Au(111) substrates used in the present study were prepared by vacuum deposition of gold on mica sheets.[3,22] The SAM was formed by immersing the gold film into a 1×10^{-3} mol dm^{-3} ethanol solution of the thiol for 24 h. A gold substrate was then rinsed with ethanol and dried in air. In situ STM and voltammetry were carried out in a 0.5 mol dm^{-3} KOH solution with a Ag/AgCl (satd. KCl) and a platinum wire as a reference electrode and a counter electrode, respectively.

Figure 1 shows a cyclic voltammogram for the reductive desorption of a SAM composed of MESA. A sharp reduction peak of the adsorbed MESA appeared at –600 mV in the cathodic scan. Unlike the case of the long-chain alkanethiol SAMs, the peak corresponding to the reoxidation of the thiols was absent in the reverse scan, showing that the desorbed molecules were dissolved into the bulk of the solution as in the case of SAMs of COOH-terminated thiols.[6]

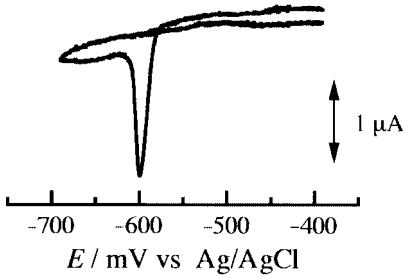

Figure 1. Cyclic voltammogram for the reductive desorption of the SAM of MESA. Scan rate: 2 mV s^{-1}.

Figure 2 shows STM images obtained in a 0.5 mol dm^{-3} KOH aqueous solution. The images were sequentially taken in the same area of 250 nm × 250 nm. STM images obtained at –200 mV and –550 mV showed no marked change in the surface structure. The STM image shown in Figure 2a was taken at –550 mV which is more positive than the potential of the reductive desorption peak of the MESA SAM. Many pits that are commonly seen in the STM images of alkanethiol SAMs were distributed on the surface. Figure 2b shows the subsequent scan of Figure 2a. The potential was stepped from –550 mV to –575 mV at the point shown by arrows during the scan from the bottom to the top. The image drastically changed in response to the potential step. The morphological change of the surface observed in Figure 2b is clearly associated with the reductive desorption of the SAM, as –575 mV corresponds to the rising foot of the reductive desorption peak shown in Figure 1.[6] Three characteristic features in the image after the potential step (upper part of Figure 2b) are i) the flatness of the imaged area, ii) the appearance of islands observed as bright spots (shown by large arrows) having the height which is about ten times larger than that of the single step of Au(111), and iii) the presence of pits especially observed immediately after the potential step (shown by small arrows). The pits appeared after the potential step are attributable to those existed before the potential step. The rapid disappearance of the pits at the upper part of the image suggests that the pits quickly diffuse away to the terrace edges after the SAM desorption.

The subsequent three images (Figure 2c–e) were taken while the potential was kept at –575 mV. The brighter regions appeared around the edge of the defect of Au(111)[10,23] at the upper right in Figure 2c (shown by arrow). The rest of the image is composed of the flat area. In Figure 2d, the areas where the brighter regions were observed extended to over the half of the terrace and exhibited striped pattern. The stripes extended further and covered about two thirds of the image in Figure 2e. The magnified image (Figure 2f) shows that the stripe consists of two bright lines. The distance between the stripes is 6.5 nm which is consistent with

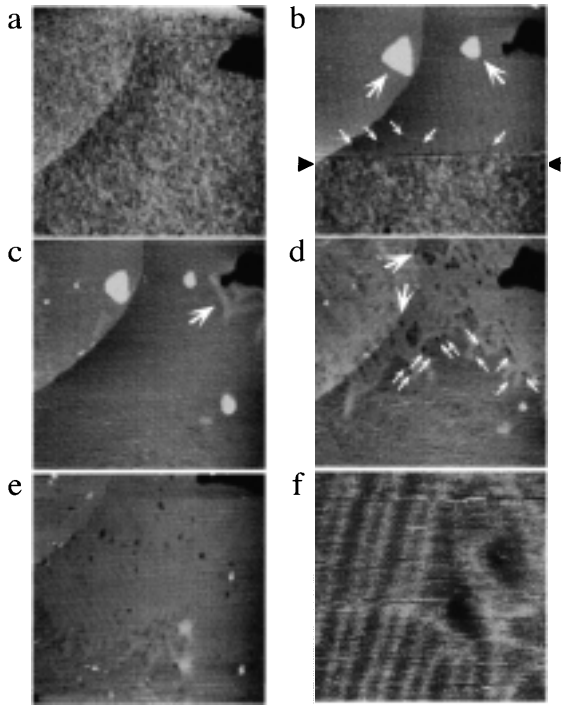

Figure 2. STM images of the Au surface taken in a 0.5 M KOH solution a) at –550 mV, b) at –550 mV (lower part) and at –575 mV (upper part), c) at –575 mV after ~2 min from the potential step in Figure 2b), d) at –575 mV after ~4 min from the potential step, and e), f) at –575 mV after ~10 min from the potential step. All images were obtained in the constant current mode with a Pt–Ir tip coated with apiezon wax. Scan size: a) – e) 250 nm × 250 nm, f) 40 nm × 40 nm. Tip potential: +50 mV vs Ag/AgCl.

previous STM images of the reconstructed Au(111).[10] It seems, therefore, that the region where the stripes were observed is reconstructed into the $(\sqrt{3} \times 23)$ structure and the flat region is the (1×1) structure of Au(111).

In Figure 2c, both two islands which observed in Figure 2b shrunk in size and decreased in height. In Figure 2d, the two islands in Figures 2b and 2c completely disappeared although several islands whose size was less than 8 nm in diameter remained at different positions. The islands are likely to be the aggregates of the reduced MESA molecules. The gradual shrinking of the islands seems to reflect the process of dissolving the aggregates of MESA into the bulk of the solution. The instantaneous appearance of the aggregates suggests the sharp phase transition of the MESA SAM.[6]

It is noteworthy that the pits whose size is about 3 nm in diameter appeared especially at the boundaries between the unreconstructed and the reconstructed areas in Figure 2d (shown by small arrows). It can be seen from the comparison between Figures 2d and 2e that some of the pits observed in Figure 2d disappeared and some of those remained on the terrace, suggesting the pits are mobile on the reconstructed surface. The appearance of the pits on the terrace of Au(111) during the progress of the reconstruction indicates that the partial source of the 4.4% of extra amount of gold atoms required for the formation of the reconstructed surface[15] is the atoms on the terrace. The rest of the extra atoms required for the reconstruction come from the terrace edges because the total area of the pits in the reconstructed region is less than 4.4% (2.6 ± 0.6% in the case of Figure 2c). This is supported by the fact that the shape of the terrace edges (indicated by large arrows in Figure 2d) was changed after the reconstruction. The partial disappearance of the pits indicates the diffusion of the pits. The rate of the diffusion is, however, slower than that of the pits in Figure 2b, suggesting that the pits in the reconstructed region were stabilized by the reconstruction.

In conclusion, the (1×1) structure is attained immediately after the reductive desorption of the SAM. The reconstruction gradually occurs in the time scale of several minutes, which is consistent with the STM imaging of Au(111) in a $HClO_4$ solution.[10,23] The pits on the (1×1) surface, i.e., those that are present before the desorption of the SAM, quickly disappeared after the desorption. On the other hand, the pits on the reconstructed surface, i.e., those that are formed by the transition from unreconstructed to reconstructed surfaces have longer life time. The reconstruction after the desorption of SAMs might be related to the small peak that sometimes appears at potentials slightly more negative than the main desorption peak.[6,24]

This work was partially supported by a grant from Foundation Advanced Technology Institute (D. H.), Grant-in-Aid for Encouragement of Young Scientists No. 12750731 from the Ministry of Education, Science, Sports, and Culture of Japan (D. H.), and CREST of JST (Japan Science and Technology) (D. H. and T. K.).

References and Notes

1 C. A. Widrig, C. Chung, and M. D. Porter, *J. Electroanal. Chem.*, **310**, 335 (1991).
2 D. E. Weisshaar, B. D. Lamp, and M. D. Porter, *J. Am. Chem. Soc.*, **114**, 5860 (1992).
3 S. Imabayashi, M. Iida, D. Hobara, Z. Q. Feng, K. Niki, and T. Kakiuchi, *J. Electroanal. Chem.*, **428**, 33 (1997).
4 B. D. Lamp, D. Hobara, M. D. Porter, K. Niki, and T. M. Cotton, *Langmuir*, **13**, 736 (1997).
5 M. Nishizawa, T. Sunagawa, and H. Yoneyama, *J. Electroanal. Chem.*, **436**, 213 (1997).
6 D. Hobara, K. Miyake, S. Imabayashi, K. Niki, and T. Kakiuchi, *Langmuir*, **14**, 3590 (1998).
7 U. Harten, A. M. Lahee, J. P. Toennies, and C. Woll, *Phys. Rev. Lett.*, **54**, 2619 (1985).
8 M. A. Van Hove, R. J. Koestner, P. C. Stair, J. P. Biberian, L. L. Kesmodel, I. Bartos, and G. A. Somorjai, *Surf. Sci.*, **103**, 189 (1981).
9 W. Haiss, D. Lackey, K. Sass, and K. H. Besocke, *J. Chem. Phys.*, **95**, 2193 (1991).
10 X. Gao, A. Hamelin, and M. J. Weaver, *J. Chem. Phys.*, **95**, 6993 (1991).
11 D. Hobara, T. Sasaki, S. Imabayashi, and T. Kakiuchi, *Langmuir*, **15**, 5073 (1999).
12 S. Imabayashi, D. Hobara, T. Kakiuchi, and W. Knoll, *Langmuir*, **13**, 4502 (1997).
13 D. D. Chambliss, R. J. Wilson, and S. Chiang, *J. Vac. Sci. Technol. B*, **9**, 933 (1991).
14 M. Hara, H. Sasabe, and W. Knoll, *Thin Solid Films*, **273**, 66 (1996).
15 G. E. Poirier, *Langmuir*, **13**, 2019 (1997).
16 A. S. Dakkouri, D. M. Kolb, R. Edelstein-Shima, and D. Mandler, *Langmuir*, **12**, 2849 (1996).
17 M. J. Giz, B. Duong, and N. J. Tao, *J. Electroanal. Chem.*, **465**, 72 (1999).
18 H. Hagenström, M. A. Schneeweiss, and D. M. Kolb, *Langmuir*, **15**, 2435 (1999).
19 T. Sawaguchi, F. Mizutani, and I. Taniguchi, *Langmuir*, **14**, 3565 (1998).
20 R. Yamada and K. Uosaki, *Langmuir*, **14**, 855 (1998).
21 S. Yoshimoto, N. Hirakawa, K. Nishiyama, and I. Taniguchi, *Langmuir*, **16**, 4399 (2000).
22 D. Hobara, M. Ota, S. Imabayashi, K. Niki, and T. Kakiuchi, *J. Electroanal. Chem.*, **444**, 113 (1998).
23 D. M. Kolb, *Progress Surf. Sci.*, **51**, 109 (1996).
24 C.-J. Zhong and M. D. Porter, *J. Electroanal. Chem.*, **425**, 147 (1997).